

RESEARCH ARTICLE

Heterozygous Nonsense Mutation *SATB2* Associated With Cleft Palate, Osteoporosis, and Cognitive Defects

Petcharat Leoyklang,¹ Kanya Suphapeetiporn,¹ Pichit Siriwan,² Tayard Desudchit,¹ Pattraporn Chaowanapanja,³ William A Gahl,⁴ and Vorasuk Shotelersuk^{1*}

¹Department of Pediatrics, Chulalongkorn University, Bangkok, Thailand; ²Department of Surgery, Chulalongkorn University, Bangkok, Thailand; ³Department of Radiology, Faculty of Medicine, Chulalongkorn University, Bangkok, Thailand; ⁴Section on Human Biochemical Genetics, Medical Genetics Branch, National Human Genome Research Institute, National Institutes of Health, Bethesda, Maryland

Communicated by Iain McIntosh

Studies of human chromosomal aberrations and knockout (KO) mice have suggested *SATB2* as a candidate gene for a human malformation syndrome of craniofacial patterning and brain development. Of 59 unrelated patients with craniofacial dysmorphism, with or without mental retardation, one 36-year-old man had a nonsynonymous mutation in *SATB2*. The affected individual exhibited craniofacial dysmorphisms including cleft palate, generalized osteoporosis, profound mental retardation, epilepsy and a jovial personality. He carries a de novo germline nonsense mutation (c.715C>T, p.R239X) in the exon 6 of *SATB2*. Expression studies showed that the mutant RNA was stable, expected to produce a truncated protein predicted to retain its dimerization domain and exert a dominant negative effect. This new syndrome is the first determined to result from mutation of a gene within the family that encodes nuclear matrix-attachment region (MAR) proteins. *Hum Mutat* 28(7), 732–738, 2007. Published 2007 Wiley-Liss, Inc.†

KEY WORDS: *SATB2*; cleft palate; osteoporosis; cognitive deficit; epilepsy

INTRODUCTION

Cleft palate has various known and suspected genetic etiologies in humans [Stanier and Moore, 2004; Park et al., 2006]. One possibly causative gene is *SATB2*, encoding a cell type-specific transcription factor that functions as a regulator of the transcription of large chromatin domains. Unlike classic transcription factors that bind individual target genes to regulate transcription, *SATB2* binds to multiple sites, influencing chromatin organization and structure and orchestrating the transcription of several genes. *SATB2* is a target for SUMOylation, a reversible protein modification that modulates its activity as a transcription factor [Dobrev et al., 2003]. The *SATB2* (MIM# 608148) gene resides on chromosome 2q32–q33, spans 191 kb, and contains 11 exons. Its open reading frame begins in exon 2, with the first stop codon in exon 11, predicting a 733–amino acid protein. The protein contains a Pfam-B_10016 domain required for dimerization (residues 57–231), two CUT domains (352–437 and 482–560), and a homeodomain (614–677) [FitzPatrick et al., 2003].

Diverse evidence links *SATB2* to the occurrence of cleft palate. Rodent studies indicate that *Satb2* plays an important role in craniofacial patterning [Britanova et al., 2006b; Dobrev et al., 2006], and brain development [Britanova et al., 2005, 2006a; Szemes et al., 2006]. Two patients with isolated cleft palate and balanced chromosomal translocations had disruptions in *SATB2* [FitzPatrick et al., 2003]. Four other patients exhibited the combination of cleft or high palate and interstitial deletions at 2q32–q33 [Van Buggenhout et al., 2005]. In Singaporean and Taiwanese patients, SNPs in the *SATB2* gene have been found in significant association with isolated cleft lip and palate [Beaty

et al., 2006]. Despite these findings, mutation analysis has failed to identify a definitive intragenic *SATB2* mutation in any individual with an isolated oral cleft [FitzPatrick et al., 2003; Vieira et al., 2005]. Consequently, we examined the *SATB2* gene in 59 individuals with craniofacial dysmorphism with or without mental retardation. One member of this group, with craniofacial dysmorphism and profound mental retardation, carries a de novo nonsense mutation in *SATB2*.

PATIENTS AND METHODS

Patients

A total of 59 unrelated patients were studied under the auspices of the Thai Red Cross, a national charity organization devoted to providing clinical care for the poor. Subjects were recruited between 1999 and 2006 from 15 medical centers throughout Thailand. The study was approved by the local Ethics Committee;

Received 15 November 2006; accepted revised manuscript 5 February 2007.

*Correspondence to: Professor Vorasuk Shotelersuk, M.D., Division of Medical Genetics and Metabolism, Department of Pediatrics, Sor Kor Building 11th floor, King Chulalongkorn Memorial Hospital, Bangkok 10330, Thailand. E-mail: vorasuk.s@chula.ac.th

Grant sponsors: Chulalongkorn University Research Unit Grant; National Center for Genetic Engineering and Biotechnology; Thailand Research Fund.

DOI 10.1002/humu.20515

Published online 21 March 2007 in Wiley InterScience (www.interscience.wiley.com).

†This article is a US government work and, as such, is in the public domain in the United States of America.

written informed consent was obtained from each person included in the study.

Clinical Studies

For the proband, a CT scan of facial bones was performed with Somatom sensation 16 scanner (Siemens, Forchheim, Germany). The images were obtained using a soft tissue and bone algorithm with 0.75-mm thin collimation, spiral technique. The scan covers the vertex to the inferior aspect of the mandible. Axial, coronal, sagittal, and three-dimensional (3D) images were reconstructed. An MRI of the brain was performed using GE Signa Excite 1.5 Tesla (GE, Fairfield, CT). The imaging protocols were spin echo spin lattice relaxation time-weighted imaging (SE T1WI), fast spin echo spin spin relaxation time-weighted imaging (FSE T2WI), gradient recalled echo spin-spin interaction time plus magnetic field inhomogeneities and susceptibility effects-weighted imaging (GRE T2*WI), fluid attenuation inversion recovery (FLAIR) imaging, echo planar imaging (EPI) diffusion-weighted imaging, and post-contrast SE T1WI with intravenous injection of gadolinium 0.1 mmol/kg. An overnight video-electroencephalography (EEG) was performed on a 32-channel digital video-EEG machine (Stellate, Montreal, Quebec, Canada) with spike detector. Total duration of the study was 12 hr.

Mutation Analysis

Genomic DNA was isolated from peripheral blood, obtained at the time of blood typing and hematocrit determination, according to established protocols. Intronic primers were used to amplify fragments encompassing exons 2–11 of the *SATB2* gene (Table 1). PCR reactions were carried out in a 20 μ L volume containing 50 ng genomic DNA, 1 \times PCR buffer, 1.5 mM MgCl₂, 0.2 mM dNTPs, 0.2 μ M of each primer, and 0.5 unit Taq polymerase, using the following parameters: 30 s at 94°C, 30 s at the annealing temperature (Table 1), and 30 s at 72°C for 35 cycles. PCR products were treated with ExoSAP-IT (USP Corporation, Cleveland, OH) according to the manufacturer's recommendations, and sent for direct sequencing at MacroGen Inc. (Seoul, Korea). Analyses were performed by Sequencher 4.2 (Gene Codes Corporation, Ann Arbor, MI). When the results indicated a possible new variant, the sample was resequenced. The position of mutations corresponds to the coding sequence for *SATB2* (RefSeq NM_015265.1), with +1 corresponding to the A of the ATG translation initiation codon.

Restriction Enzyme Analysis

The nonsynonymous coding variant was verified by restriction enzyme digestion of the patient's PCR products. *SATB2* exon 6

was PCR-amplified using a mutagenic forward primer to incorporate a *Bss*SI recognition site, 5' TAATTATCACTTT TATCTCTT AACAGTGGAAAGAGTGGCA 3', and a reverse primer, 5'-TGTCCCTGAGATCCATAAAAGC-3'. The PCR conditions were 30 s at 94°C, 30 s at 57°C, and 30 s at 72°C for 35 cycles. The PCR products were digested with *Bss*SI according to the manufacturer's specifications (New England Biolabs, Ipswich, MA) and electrophoresed on a 3% agarose gel stained with ethidium bromide.

The proband's parents were examined for the variant by sequencing and restriction enzyme analysis. Paternity and maternity were confirmed by typing 15 microsatellite markers on 13 different chromosomes (data not shown). Thai control individuals (n = 105) were analyzed by restriction enzyme analysis.

RNA Studies

Total RNA was isolated from white blood cells using a QIAamp[®] RNA blood mini kit (Qiagen, Valencia, CA). Reverse transcription was performed using ImProm-II[™] reverse transcriptase (Promega, Madison, WI), according to the company's recommendations. PCR amplification of the *SATB2* cDNA partial exons 5 and 6 was performed using primers cDNA-F4, 5'-CCAATGTGTCAGCAACCAAG-3' and cDNA-R1, 5'-TGGT GAATTTGGCTGTGAGG-3'. We used 2 μ L of first-strand cDNA, 1 \times PCR buffer, 1.5 mM MgCl₂, 0.2 mM dNTPs, 0.5 μ M of each primer, and 0.5 U Taq DNA polymerase in a total volume of 20 μ L. The PCR conditions were 30 s at 94°C, 30 s at 60°C, and 30 s at 72°C for 26, 28, 30, 32, 35, 37, 40, or 42 cycles. The 199-bp PCR products were treated with ExoSAP-IT and subjected to direct sequencing.

RESULTS

Case Report

The patient is a 36-year-old man born at term by vaginal delivery to a 24-year-old, gravida 3, para 2 mother and a 32-year-old unrelated father. The pregnancy and labor were uncomplicated. Cleft palate was apparent in infancy, but was not surgically corrected. The patient walked at 4 years of age and could speak a single word, "nee," meaning mother, from 6 years of age. He had several febrile seizures during childhood and developed generalized tonic-clonic seizures at age 26 years. His mother reported that he had frequent and severe respiratory tract infections during childhood, worse than those of his three unaffected siblings. At age 35, while walking, the patient fell and fractured his left tibia, left fibula, and right third metatarsus. He required assistance for daily routines including dressing, washing, and eating. His mood was jovial. Physical examination at age 36 years revealed a height of

TABLE 1. Oligonucleotides and PCR Condition for *SATB2* Mutation Analysis

Primer sequences for PCR (5' to 3')				
Exon	Forward	Reverse	Annealing temperature (°C)	Product size (bp)
2	GTCCCTGTGCGTTTTATTGC	GCAACCTGGAATTCCTTCC	57	350
3	TGTTGCTTCCCTTCTCATCG	TACTGCTCACTAGGAAATGC	57	390
4	AATATCTGAGTGGGCCTTGG	CAGGACATGCTGATCTTTGC	59	330
5	AGCAATTTCTCTGAAGCTCC	ACAGTTGTTTAAGCAGAAGG	55	325
6	TAGTGCAGGTTATAAAGTGC	TTTTAAGGGAGCCAATAGG	55	352
7	ACTTTTATGCTGGAGCTTCC	TGTCCTGAGATCCATAAAGC	55	725
8	TGTGAGGTTCTTGACATCAC	GTCTCTCAATGTTGAGGGA	55	431
9	GCATCAGCTGACTGAAATCC	GAACATGACAGGTTTCTTGG	57	379
10	ATGTACTGTGATGGCACTGG	GAAGTTGGTGTGGTGTGTC	59	383
11	AATGACTATAGCTTACCTCC	TGAAAGCAGAAAATCCTTGG	55	632

165 cm (25th centile), weight 40 kg (less than third centile), and head circumference 56 cm (50th centile). He had gum hyperplasia, slight micrognathia, and deviation of the chin to the right (Fig. 1A and B). His chest, abdomen, genitalia, and extremities were unremarkable.

Blood counts, urinalysis, blood urea nitrogen (BUN), creatinine (Cr), electrolytes, chromosomal analysis, immunoglobulin (Ig) G, IgM, IgA, and IgE were all within normal ranges. Plain radiographs of his facial bones, chest, hands, legs, feet, spine, and urinary system showed generalized osteoporosis, narrow bilateral carpometacarpal and tarsometatarsal joints (Fig. 1I), loss of normal kypholordotic curvature of the thoracolumbar spine (not shown), and anterior bowing of the tibiae (Fig. 1J). Old healed fracture lines were observed at the proximal left fibular shaft, the distal left

tibial shaft, and the lateral side of the midright third metatarsal shaft.

A CT scan of the facial bones revealed bilateral asymmetric mandibular hypoplasia (Fig. 1C), wide mandibular angles, anterior overbite of the upper teeth with marked anterior-pointing incisors (Fig. 1D), a midline cleft palate, small sizes and abnormal shapes of the bilateral maxillary sinuses (Fig. 1E), and mild ocular hypertelorism with the anterior and midinterorbital distances measuring 30.9 mm (normal range: 19.9–27.7 mm) and 34.0 mm (normal range: 22.3–32.7 mm), respectively (Fig. 1F). [Waitzman et al., 1992] In addition, slightly short zygomatic arches were observed, and the mandibular condylar heads were flattened rather than oval (not shown). A brain MRI showed no demonstrable intracranial abnormality (Fig. 1G). However, cervical spine imaging revealed a hyperintense mass on T2-weighted image at the right side of C3-4 vertebrae (Fig. 1H), considered an incidental finding.

An awake EEG revealed a background of bilateral symmetrical 8 to 9 Hz, 50 to 75 μ V waves, attenuated by eye opening. The sleep EEG revealed a mix of generalized, irregular, slow 2 to 3 Hz, 25 to 50 μ V waves and 4 to 5 Hz, 25 to 50 μ V waves. Bilateral synchronous sleep spindles, 12 to 13 Hz, 50 to 75 μ V waves and vertex transient, 75 to 100 μ V waves, were noted in the paracentral head areas. Multiregional sharp waves phase reversing at T3, T5, T4, T6, C3, and C4 every 2 to 5 minutes were found (Fig. 2). Occasionally, these sharp waves spread and lateralized to the right and left hemispheres. Rare short runs of repetitive spikes were seen. No clinical or EEG seizures occurred during the period of recording.

Molecular Analyses

Of 59 patients investigated with craniofacial dysmorphism, one exhibited an alteration in the coding region of *SATB2*. The mutation was a c.715C>T transition in exon 6 (Fig. 3A), converting an arginine (CGA) into a premature TGA stop codon (p.R239X). Each parent had only the wild-type allele, indicating that the patient's c.715C>T mutation occurred de novo. No other sequence variants were found in the patient's *SATB2* coding regions. Leukocyte mRNA of the *SATB2* gene, quantitated by reverse transcription and PCR sequencing after 32 cycles of PCR,

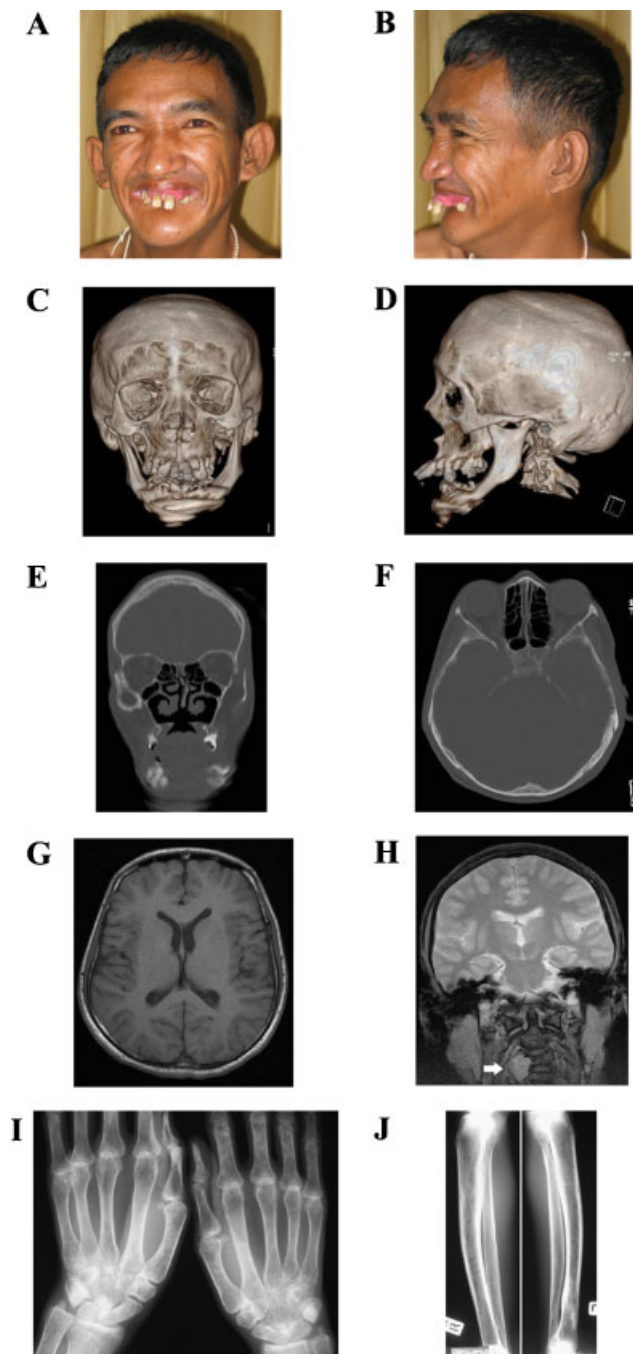


FIGURE 1. Clinical features and imaging studies of the patient with a *SATB2* nonsense mutation. **A,B:** Craniofacial features of the patient, anterior and lateral views, respectively. **C,D:** Reconstructed images of the CT scan of facial bones, anterior and lateral views, respectively. Note the anterior open bite with marked anterior-pointing incisors. Shallow mandibular notches and wide mandibular angles reflect mandibular hypoplasia, which is more severe on the right resulting in right-sided pointed chin. Motion artifacts are seen at the mid-body of mandible causing irregular blur image. **E:** The coronal plane, bone window of the CT scan of facial bones. A 2-cm wide, midline cleft palate and absent vomer are seen. Note the small size and abnormal shape of the bilateral maxillary sinuses, high position of the inferior maxillary walls and wide inferior meati bilaterally. **F:** The axial plane, bone window of the CT scan of facial bones demonstrating mild hypertelorism. **G:** An axial T1WI of the MRI of the brain with no demonstrable abnormalities of the brain parenchyma. **H:** A T2WI of the MRI of the brain demonstrating a 2.3 \times 1.9 cm hyperintense mass at the right side of C3-4 vertebrae (arrow). **I,J:** Plain radiographs of the wrists in anteroposterior view and legs in lateral view demonstrating narrowing of carpometacarpal joints and anterior bowing of both tibiae, respectively. [Color figure can be viewed in the online issue, which is available at www.interscience.wiley.com.]

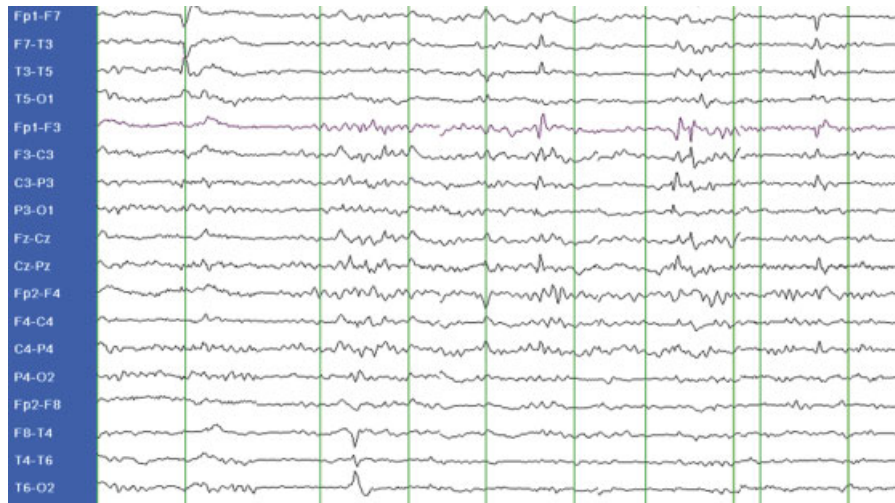
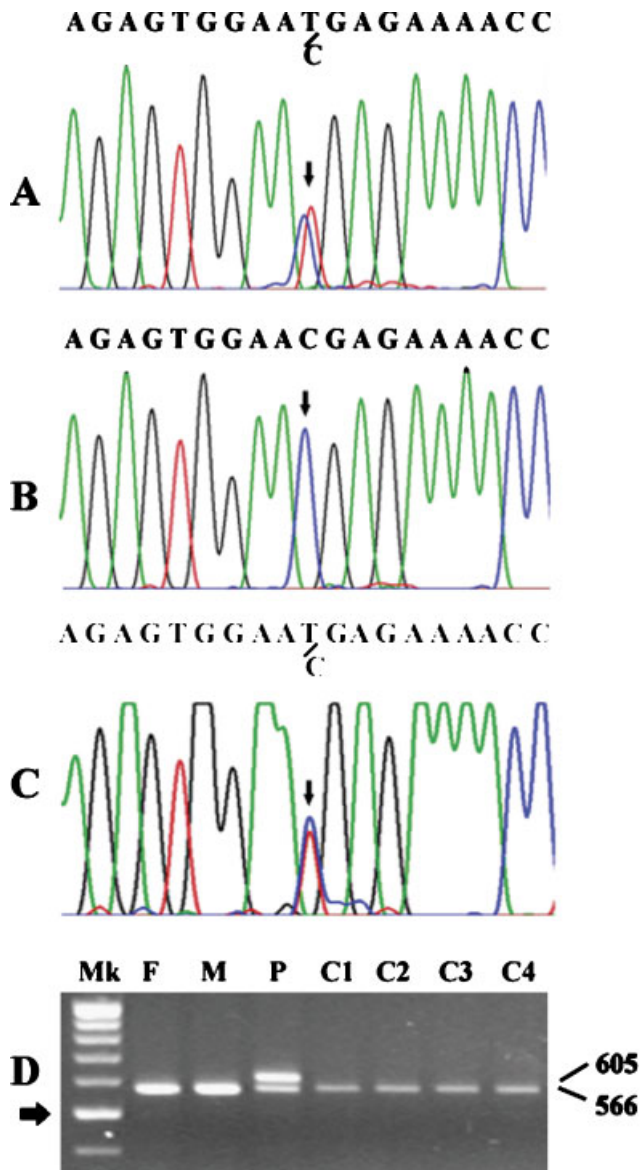


FIGURE 2. A composite picture of the electroencephalogram demonstrates multiregional sharp waves phase reversing at T3, T5, T4, T6, C3, and C4, with sharp waves lateralized to the left hemisphere. [Color figure can be viewed in the online issue, which is available at www.interscience.wiley.com.]



while in the exponential phase (data not shown), was present in equivalent amounts for the mutant and wild-type alleles (Fig. 3C).

The c.715C>T transition was confirmed by digestion of the PCR products using a mutagenic primer with the restriction enzyme *BssSI*, whose recognition site was removed by the point mutation (Fig. 3D). The mutation was not previously reported and was not detected in 105 control individuals (210 alleles).

DISCUSSION

Studies of human chromosomal aberrations and knockout (KO) mice have suggested *SATB2* as a candidate gene for human malformation syndromes involving abnormalities in craniofacial patterning and brain development. This led us to investigate *SATB2* in individuals with craniofacial malformations with or without mental retardation. We identified the first human individual having a pathogenic *SATB2* point mutation. He had craniofacial dysmorphism, generalized osteoporosis, profound mental retardation, epilepsy, and a pleasant personality.

Our patient's clinical features are similar but not identical to those of model mice and other syndromic patients (Table 2). His craniofacial dysmorphisms, including maxillary malformation, mandibular hypoplasia, and cleft palate, resembled those of mice lacking *Satb2* [Dobrev et al., 2006]. The asymmetric mandibular hypoplasia in our patient is consistent with the asymmetric snout of adult heterozygous *Satb2*^{+/-} mice [Britanova et al., 2006b].

FIGURE 3. *SATB2* gene mutation. **A,B**: DNA sequence analyses of *SATB2* from the patient and his father, respectively. The arrows indicate the heterozygous mutation, T/C, in the patient and the wild-type only, C, in the father. **C**: The patient's leukocyte RNA sequence analysis. The arrow indicates the mutant base, T, is present in an amount equal to that of the wild-type base, C. **D**: Restriction enzyme analysis. With a mutagenic primer, the mutant allele in the patient (P) eliminates the *BssSI* recognition site resulting in an uncut 605-bp band, presenting along with a 566-bp band of the wild-type allele. The 39-bp band of the cut wild-type allele is not visible. The patient's father (F), mother (M), and controls (C) have only the wild-type allele. The 500-bp band of the 100-bp marker (M) is indicated by an arrow. [Color figure can be viewed in the online issue, which is available at www.interscience.wiley.com.]

TABLE 2. Characteristics of Our Patient Compared With Those of *SATB2* KO Mice, Patients With Chromosomal Abnormalities Involving *SATB2*, and Patients With Known Syndromes Including Cleft Palate, Osteoporosis, and Mental Retardation

	Our patient	<i>SATB2</i> KO mice [Britanova et al., 2006b; Dobрева et al., 2006]	Patients with chromosomal translocation interrupting <i>SATB2</i> [Brewer et al., 1999]	del(2)(q32.2q33) deletion syndrome [Van Buggenhout et al., 2005]	Snyder-Robinson syndrome (MIM# 309583)	Larsen syndrome (MIM# 245600)	Lowry-Maclean syndrome (MIM# 600252)	Rothmund-Thomson syndrome (MIM# 268400)
Microcephaly	A	P	A	P	A	A	P	A
Cleft palate	P	P	P	P	P	P	P	P
Other craniofacial dysmorphism	Hypertelorism, short zygomatic arches, anterior overbite, gum hyperplasia, asymmetric mandibular hypoplasia, wide mandibular angle	Truncation of mandible, shortening of nasal and maxillary bones, missing incisor teeth, small tongue	Long narrow face, hypotelorism, squint, prominent nasal bridge, underhanging columella, small mouth, micrognathia	Thin hair, high nasal bridge, micrognathia, macroglossia, maxilla hypoplasia	Facial asymmetry	Small face, prominent forehead, hypertelorism, glaucoma, beaked nose bridge	Craniosynostosis, glaucoma, delayed dentition, beaked nose	Alopecia, frontal bossing, prognathism, cataracts, microphthalmia, small nose, microdonia
Stature	Normal	NA	Normal	Short	Tall	Short	Short	Short
Mental retardation	Profound	NA	Mild delayed development	Severe	Mild to moderate	P	P	P
Epilepsy	P	NA	A	P	P	A	A	A
Osteoporosis	P	P	NA	NA	P	P	P	P
Personality-behavior	Happy	NA	NA	Happy, aggression, anxiety	NA	NA	NA	NA
Others	Narrow carpometacarpal and tarsometatarsal joints	Died immediately after birth	Long and slender fingers	Inguinal hernia, wide-based gait, sleep problems, self-mutilation	Hypotonia, unsteady gait, marfanoid habitus, kyphoscoliosis, cryptorchidism	Dislocation of joints, club feet, scoliosis, skin laxity, hypotonia	Eventration of diaphragm, congenital heart defect	Forearm reduction, small hands and feet, poikiloderma, photosensitivity, ectodermal dysplasia
Mutated gene	<i>SATB2</i>	<i>Satb2</i>	<i>SATB2</i>	NA	SMS	Unknown	Unknown	<i>RECQL4</i>
Chromosome	2q32	NA	2q32	2q32-q33	Xp22	Unknown	Unknown	8q24

A, absent; P, present; NA, not applicable or not available.

abnormal craniofacial patterning in *Satb2* KO mice involves desuppression of the *Hoxa2* expression. *Hoxa2* inhibits bone formation, and *Satb2* suppresses *Hoxa2* expression, so the absence of *Satb2* inhibits osteoblast differentiation [Ellies and Krumlauf, 2006]. Craniofacial development is sensitive to *Satb2* dosage, with full functional loss resulting in amplification of the defects seen in *Satb2* haploinsufficiency [Britanova et al., 2006b]. Our patient's craniofacial abnormalities are more severe than those associated with the *SATB2* haploinsufficiency of 2q32–q33 deletions and translocations, perhaps due to the possible dominant negative nature of his mutation. In addition to abnormal skeletal patterning, generalized osteoporosis and fractures occurred in our patient, consistent with the proposed role of *SATB2* in regulating skeletal development and osteoblast differentiation [Dobrev et al., 2006].

Our patient also has profound mental retardation and epilepsy. *Satb2* is expressed in mouse and rat developing neocortex and is involved in the control of neuronal differentiation and migration [Britanova et al., 2005, 2006a; Szemes et al., 2006]. Our patient has a normal head circumference, whereas the *Satb2*^{+/-} mice were microcephalic, with increased microcephaly in *Satb2*^{-/-} [Britanova et al., 2006b]. The two patients with translocations involving *SATB2* haploinsufficiency had mild learning disability in addition to cleft palate [FitzPatrick et al., 2003]. Our patient's pleasant personality resembles that of patients with the del(2)(q32.2q33) interstitial deletion syndrome [Van Buggenhout et al., 2005].

SATB2 regulates expression of the immunoglobulin mu gene [Dobrev et al., 2003], and the patient had frequent respiratory tract infections, but his immunoglobulin levels, including IgM, were normal. The hyperintense mass at the right side of our patient's C3-4 vertebrae was thought to be a schwannoma, mesenchymal tumor, or an expansile benign bony tumor; the relationship to *SATB2* mutations requires further investigation. Since chromosomal aberrations affect many different genes, the contribution of *SATB2* mutations to the phenotypes of patients with chromosomal translocations and interstitial deletions is not known. A T190A mutation in *SATB2* has recently been identified in a Filipino patient with isolated bilateral cleft lip and cleft palate. Although not found in 186 matched controls and in a panel of 1,064 Centre d'Etude du Polymorphisme Humain (CEPH) controls, this mutation involves a base that is not highly conserved across species, is predicted to be benign by PolyPhen (www.bork.embl-heidelberg.de/PolyPhen; Peer Bork EMBL, Heidelberg, Germany), and was present in his unaffected mother. The presence of only cleft palate and not cleft lip in our patient, in individuals with chromosomal aberrations involving *SATB2*, and in *Satb2* KO mice makes the etiologic role of the *SATB2* T190A mutation further suspect. In contrast, the pathogenic role of our patient's c.715C>T mutation in *SATB2* is supported by three lines of evidence. First, this nonsense mutation is expected to result in a truncated protein of 238 residues, instead of 733 residues, lacking the two functional CUT domains and homeodomain. Second, his molecularly-confirmed biological parents had only wild-type alleles, indicating that the mutation is de novo. Third, the mutation was absent from 105 ethnically-matched control individuals. Therefore, the c.715C>T mutation is the first definitive intragenic mutation of *SATB2* in a human; a previous of 70 unrelated isolated cleft palate patients failed to identify any pathogenic *SATB2* mutations [FitzPatrick et al., 2003].

The presence of the mutant RNA in our patient's leukocytes indicated lack of nonsense-mediated mRNA decay. Rather, translation is predicted to produce a truncated protein of 238 residues retaining its dimerization domain (residues 57–231).

Nevertheless, impaired function could result in haploinsufficiency. With respect to the mechanism of the defect involved, it should be noted that the transcripts used in our study were from adult leukocytes, while *SATB2* acts early in development; the transcript levels should be interpreted with caution. As more patients with *SATB2* mutations are recognized, the syndrome will be better defined. Patients with phenotypes similar to that of our patient (Table 2), but with an unidentified causative gene, should be considered candidates for *SATB2* mutation analysis.

ACKNOWLEDGMENTS

We thank the medical staff of the Thai Red Cross and the Provincial Hospitals of Nakornratchaseema, Srakaew, Uthaitanee, Nan, Maehongsorn, Trang, Prachinburi, Kalasin, Nongkhai, Maharakam, Chaiyapoom, Leoy, Yasothorn, and Mukdaharn for the excellent care of their patients. We are indebted to Dr. Pornarun Sirichotvithyakorn for her expertise in anesthesia for the patient required for imaging studies.

REFERENCES

- Beatty TH, Hetmanski JB, Fallin MD, Park JW, Sull JW, McIntosh I, Liang KY, Vanderkolk CA, Redett RJ, Boyadjev SA, Jabs EW, Chong SS, Cheah FS, Wu-Chou YH, Chen PK, Chiu YF, Yeow V, Ng IS, Cheng J, Huang S, Ye X, Wang H, Ingersoll R, Scott AF. 2006. Analysis of candidate genes on chromosome 2 in oral cleft case-parent trios from three populations. *Hum Genet* 120:501–518.
- Brewer CM, Leek JP, Green AJ, Holloway S, Bonthron DT, Markham AF, FitzPatrick DR. 1999. A locus for isolated cleft palate, located on human chromosome 2q32. *Am J Hum Genet* 65:387–396.
- Britanova O, Akopov S, Lukyanov S, Gruss P, Tarabykin V. 2005. Novel transcription factor *Satb2* interacts with matrix attachment region DNA elements in a tissue-specific manner and demonstrates cell-type-dependent expression in the developing mouse CNS. *Eur J Neurosci* 21:658–668.
- Britanova O, Alifragis P, Junek S, Jones K, Gruss P, Tarabykin V. 2006a. A novel mode of tangential migration of cortical projection neurons. *Dev Biol* 298:299–311.
- Britanova O, Depew MJ, Schwark M, Thomas BL, Miletich I, Sharpe P, Tarabykin V. 2006b. *Satb2* Haploinsufficiency phenocopies 2q32–q33 Deletions, whereas loss suggests a fundamental role in the coordination of jaw development. *Am J Hum Genet* 79:668–678.
- Dobrev G, Dambacher J, Grosschedl R. 2003. SUMO modification of a novel MAR-binding protein, *SATB2*, modulates immunoglobulin mu gene expression. *Genes Dev* 17:3048–3061.
- Dobrev G, Chahrour M, Dautzenberg M, Chirivella L, Kanzler B, Farinas I, Karsenty G, Grosschedl R. 2006. *SATB2* is a multifunctional determinant of craniofacial patterning and osteoblast differentiation. *Cell* 125:971–986.
- Ellies DL, Krumlauf R. 2006. Bone formation: the nuclear matrix reloaded. *Cell* 125:840–842.
- FitzPatrick DR, Carr IM, McLaren L, Leek JP, Wightman P, Williamson K, Gautier P, McGill N, Hayward C, Firth H, Markham AF, Fantes JA, Bonthron DT. 2003. Identification of *SATB2* as the cleft palate gene on 2q32–q33. *Hum Mol Genet* 12:2491–2501.
- Park JW, Cai J, McIntosh I, Jabs EW, Fallin MD, Ingersoll R, Hetmanski JB, Vekemans M, Attie-Bitach T, Lovett M, Scott AF, Beatty TH. 2006. High throughput SNP and expression analyses of candidate genes for non-syndromic oral clefts. *J Med Genet* 43:598–608.
- Stanier P, Moore GE. 2004. Genetics of cleft lip and palate: syndromic genes contribute to the incidence of non-syndromic clefts. *Hum Mol Genet* 13(Spec No 1):R73–R81.
- Szemes M, Gyorgy A, Paweletz C, Dobi A, Agoston DV. 2006. Isolation and characterization of *SATB2*, a novel AT-rich DNA binding protein expressed in development- and cell-specific manner in the rat brain. *Neurochem Res* 31:237–246.

- Van Buggenhout G, Van Ravenswaaij-Arts C, Mc Maas N, Thoelen R, Vogels A, Smeets D, Salden I, Matthijs G, Fryns JP, Vermeesch JR. 2005. The del(2)(q32.2q33) deletion syndrome defined by clinical and molecular characterization of four patients. *Eur J Med Genet* 48:276–289.
- Vieira AR, Avila JR, Daack-Hirsch S, Dragan E, Felix TM, Rahimov F, Harrington J, Schultz RR, Watanabe Y, Johnson M, Fang J, O'Brien SE, Orioli IM, Castilla EE, Fitzpatrick DR, Jiang R, Marazita ML, Murray JC. 2005. Medical sequencing of candidate genes for nonsyndromic cleft lip and palate. *PLoS Genet* 1:e64.
- Waitzman AA, Posnick JC, Armstrong DC, Pron GE. 1992. Craniofacial skeletal measurements based on computed tomography: Part II. Normal values and growth trends. *Cleft Palate Craniofac J* 29:118–128.